



KfK 2668
August 1978

Analysis of Sodium-Void Experiments in ZPPR-3 Modified Phase 3 Core

T. Yoshida
Institut für Neutronenphysik und Reaktortechnik
Projekt Schneller Brüter

Kernforschungszentrum Karlsruhe

Als Manuskript vervielfältigt
Für diesen Bericht behalten wir uns alle Rechte vor

KERNFORSCHUNGSZENTRUM KARLSRUHE GMBH

KERNFORSCHUNGSZENTRUM KARLSRUHE

Institut für Neutronenphysik und Reaktortechnik
Projekt Schneller Brüter

KfK 2668

Analysis of Sodium-Void Experiments in ZPPR-3 Modified
Phase 3 Core

T. Yoshida*

* On leave from NAIG Nuclear Research Lab., Nippon Atomic
Industry Group Co. Ltd., Kawasaki, Japan

Kernforschungszentrum Karlsruhe GmbH, Karlsruhe

Abstract

An extensive series of sodium-void reactivity measurements was performed in assembly 3 of Zero Power Plutonium Reactor (ZPPR-3), a mockup of the US Demoplant. In this series, large-zone sodium-void effects are studied in detail in the presence of many singularities, namely, control rods (CRs) and control rod positions (CRPs). The Karlsruhe data-and-method have been applied to an analysis of these experiments, and the results are presented here. This work is aimed at complementing the sodium-void reactivity analysis based on the SNEAK experiments, where it is difficult to mockup a large plutonium-core of a prototype fast breeder reactor.

The following conclusions have been drawn through a comparison of the results of measurements and calculations, the latter being obtained mainly by a three-dimensional diffusion code using heterogeneously corrected group constants.

The calculations reproduce well the experiments if the voided core region is free of singularities. A typical C/E value for such a case is 1.07. Disregarding the heterogeneity correction for the fuel elements worsens the consistency leading to an increase in C/E by more than 20%. In the present study, the correction was performed with the aid of the plate-cell collision probability code KAPER. The method of calculating the diffusion coefficient for CRPs in the immediate neighborhood of a voided fuel region influences the calculated void-worth by nearly 10% at most.

When the void region includes CRPs, which are concurrently voided, the C/E value deteriorates and varies from 0.35 to 1.58, typically, depending on the way of calculating the diffusion coefficient for the CRPs. The agreement, however, can be improved considerably by correcting the reactivity worth of the sodium contained in the CRPs with the aid of experimental data ($C/E = 1.00 \pm 0.15$). This suggests that an improved way of calculating the diffusion coefficient, which gives appropriate values for both normal and voided CRPs, must be developed.

The presence of a CR in a voided core region also influences the agreement between theory and measurement. The C/E value is too large (≈ 1.30) for a core-center void including the central CR.

The correction for the worth of sodium contained in a CRP itself hardly improves the result. For the nearly-maximum-void pattern with an experimental void-worth of 1.7 β , we obtained C/E values of 1.20 (or 0.67, depending on the diffusion coefficient used for CRPs) and 0.94 before and after the correction for the singularities, respectively.

Analyse der ZPPR-3 Modified-Phase-3 Natrium-Void-Experimente

Zusammenfassung

In der kritischen Anordnung ZPPR-3 (Zero Power Plutonium Reactor, assembly 3), einem Mockup der amerikanischen Demonstrationsanlage eines natriumgekühlten schnellen Brutreaktors, wurde eine umfangreiche Serie von Messungen der Reaktivität bei Natriumverlust durchgeführt. Der Natrium-Void-Effekt wurde besonders sorgfältig für zahlreiche Konfigurationen (Kontrollstäbe (CRs), nicht besetzte Kontrollstabpositionen ("Follower"-Bereich:CRP) untersucht. Der vorliegende Bericht beschreibt die Ergebnisse der Nachrechnungen dieser Experimente, die mit den in Karlsruhe verfügbaren Daten und Methoden durchgeführt wurden. Ziel der Arbeit war eine Erweiterung des Kenntnisstandes über die Vorhersagbarkeit der Natrium-Voidreaktivität für prototypische schnelle Reaktoren. Derartige Cores, deren Geometrie und Materialzusammensetzung ähnlich denen des SNR sind, konnten in SNEAK bisher nur schwierig nachgebildet werden. Die hier gewonnenen Kenntnisse ergänzen daher die vorliegenden Erfahrungen aus der Analyse analoger SNEAK-Experimente.

Bei der Berechnung wurde hauptsächlich das dreidimensionale Diffusionsprogramm D3D eingesetzt. Bei der Bereitstellung der Gruppenkonstanten wurden Heterogenitätseffekte durch Verwendung des Stoßwahrscheinlichkeitsprogramms KAPER berücksichtigt.

Ein detaillierter Vergleich von Rechnungen und Messungen führt zu folgenden Schlußfolgerungen: 1. Der Na-Void-Effekt kann für Corebereiche, die keine Kontrollstabpositionen enthalten, gut vorhergesagt werden; typische C/E (calculation/experiment)-Werte betragen etwa 1.07. 2. Dieser Wert kann sich um mehr als 20% vergrößern, wenn die Heterogenitätskorrektur für die Brenn-

stoffzellen nicht durchgeführt wird. 3. Die Art der Bestimmung der Diffusionskonstanten für CRPs beeinflusst den gerechneten Reaktivitätswert für Natriumverlust aus dem Corebereich in der unmittelbaren Nachbarschaft der CRPs um bis 10%. 4. Die Übereinstimmung zwischen Theorie und Experiment verschlechtert sich, wenn sich in Corebereichen ohne Natrium CRPs befinden, die ebenfalls kein Natrium mehr enthalten. Je nach Bestimmungsweise der Diffusionskonstanten für CRPs ergeben sich C/E-Werte von 0.35 bis 1.58. 5. Mit Hilfe experimenteller Ergebnisse für die Reaktivitätswerte von Natrium in CRP-Bereichen kann eine Korrektur für den Einfluß der Neutronenleckage aus CRPs ohne Natrium vorgenommen werden. Dadurch ergibt sich eine deutlich verbesserte Übereinstimmung zwischen Rechnung und Messung mit C/E-Werten von 1.00 ± 0.15 . Dies verdeutlicht, daß die hier benutzte Methode zur Bestimmung der Neutronenleckage aus leeren Kanälen als Korrektur in einer Diffusionsrechnung verbessert werden muß. 6. Das Vorhandensein von Kontrollstäben (CRs) in der näheren Umgebung von Corebereichen, aus denen Natrium entfernt wurde, bewirkt ebenfalls eine Verschlechterung der Übereinstimmung zwischen berechnetem und gemessenem Na-Void-Effekt. 7. Die Übereinstimmung wird noch weiter verschlechtert, wenn man aus diesen CRs und dem benachbarten Corebereich Natrium entfernt. Eine Korrektur, ähnlich derjenigen für die CRPs, führt in diesem Fall jedoch zu keiner wesentlichen Verbesserung. Beim Voiden des zentralen Corebereichs einschließlich des zentralen Kontrollstabs ergibt sich z.B. nach Anwendung der Korrektur ein C/E-Wert von etwa 1.30. 8. Das Entfernen von Natrium aus nahezu allen Teilbereichen des Cores, die einen positiven Beitrag zum Na-Void-Effekt liefern, ergibt einen gemessenen Reaktivitätswert von 1.7 $\%$. Die zugehörigen C/E-Werte betragen 1.20 (bzw. 0.67 abhängig von der für die CRPs verwendeten Diffusionskonstanten) ohne Korrektur für den Einfluß von Kontrollstäben und/oder Followerbereichen und 0.94 bei Berücksichtigung dieser Korrektur.

Table of Content

	page
1. Introduction	1
2. General Outline of Sodium-Void Experiments in ZPPR-3	2
3. Sodium-Void Experiments in modified Phase 3 Core of ZPPR-3	3
4. Calculation Method	4
4.1 Preparation of Group Constants	4
4.2 Cell Model	4
4.3 Diffusion Coefficients	5
4.4 Reactor Calculation	7
5. Criticality Factors	9
6. Sodium-Void Reactivity Worth	11
6.1 Analysis of the Standard Sodium-Void Experiments	11
6.2 Analysis of the Reactivity Effect of Sodium Contained in Singularities (CRs and CRPs)	13
6.3 Residual Discrepancy after Correction for Singularities	15
6.4 Impact of the Delayed Neutron Fraction Data	17
7. Conclusion	18

1. Introduction

From the safety aspect of LMFBRs, sodium-void reactivity effects play an important role especially with respect to the energy release in, so called, loss of coolant accidents.

It is very difficult, however, to predict the sodium-void reactivity worth precisely, mainly because several effects partially cancel each other in it. More specifically, the cancellation occurs mainly between the slowing down and the leakage terms. The former and the latter terms themselves are very sensitive to the calculated flux spectrum, and the diffusion coefficients used, respectively. Hence the accuracy of the calculated worths is a severe test for the adopted method-and-data. To check the adequacy of the method-and-data, many series of sodium-void experiments have been conducted in critical assemblies over the world including SNEAK, ZEBRA, FCA, ZPR and ZPPR. Among them, a series performed in ZPPR-3 (a large Pu-fueled benchmark critical for the US Demonstration Plant) is one of the most extensive void-experiments, in which geometry, core volume, and atomic compositions of a typical prototype fast reactor (SNR-300 class) are well simulated. In this series of experiments, large-zone void effects are mainly studied in the presence of many singularities, namely, control rods and sodium followers (control rod positions). Presence of these singularities in sodium-voided regions complicates the analysis, and imposes a further severe check on the analysis method.

In this report, an analysis of ZPPR-3 sodium-void experiments with Karlsruhe data-and-method is presented in order to backup the sodium-void reactivity study based on the SNEAK experiments, where it is difficult to mockup a large prototype-like Pu-core.

2. General Outline of Sodium-void Experiments in ZPPR-3

The purpose of ZPPR Assembly 3 is to provide some experimental data to backup the preliminary core design of the US Demonstration Plant. Though emphasis was placed on the assessment of the worth of the control rod system, an extensive series of sodium-void experiments was also performed in its third phase core, which simulated the beginning of the burnup cycle. Detailed information on the Assembly 3 can be found in reference 1.

The experiment was carried out by voiding sodium from progressively larger zones, step by step, until 77% of the core area became sodium-free (Phase 3 experiment). After the maximum sodium-void pattern was reached, sodium was loaded back again, step by step, into the core with a different control rod insertion pattern. Minor changes occurred also at the outer core boundary and at the control rod locations. This latter step is called modified Phase 3 experiment. Though the experiment was performed by filling back sodium, the measured worths were arranged so that the steps correspond to a voiding sequence rather than a sodium filling sequence as we will see later.

In the present analysis, we mainly deal with the modified Phase 3 experiments for the following two reasons. Firstly, we can more easily see the effect of control rods and control rod positions (followers) on void reactivity, separately, because of the simpler rod loading pattern in comparison with the standard phase 3. Secondly, the modified loading pattern has a quarter symmetry*), which allows less expensive three dimensional calculations. (All sodium-void experiments are performed in a three dimensional geometry, so we can not dispense with three dimensional calculations.) An analysis of the standard phase is performed briefly to see the consistency with the modified phase, and the results are given in Appendix A.

*) Exactly speaking, the quarter symmetry is obtained only after two control rods (CR No.11 and 17 in ANL original loading map, given in ANL-RDP reports) being moved by half a pitch (2.76 cm) to the right. Hereafter, we only relate to this "modified" quarter symmetric configuration without any further remark.

3. Sodium-Void Experiments in modified Phase 3 Core of ZPPR-3

A sectional view of Assembly 3 modified Phase 3 core is shown in Fig.1 together with a vertical profile of the assembly. In this figure, drawn mainly to show the calculational model described in the next paragraph, we leave out parts of the outermost reflector zone, and of the outer-peripheral of the radial blanket. In the present report we are only interested in the sodium-void experiments performed in the core region. Hence the details of the outer-most part of the assembly are of minor significance. As one can see in this figure, inner and outer cores are composed of two and three types of fuel drawers, respectively. Cell structure and atomic composition of these five types of core drawers will be given later, when the method of cell calculation is described. Atomic compositions of the zones other than the core region are given in Table 1.

In the core described above, nearly 20 steps of sodium-voiding were carried out. Sodium-voided situation was simulated in each of these steps by replacing the sodium-filled steel cans by empty steel cans. Throughout the experiments, the height of the void region was fixed to 24 inches (\pm 12 inches from core mid-plane), which gave approximately the maximum sodium-void reactivity effect in the axial direction. Detailed description of all these steps is given in reference 2. In the present analysis, we select four typical patterns out of them, which gives us good insight into the effect of the presence of control rods and rod positions, separately. These four sodium-void patterns are shown in Fig.2. Measured reactivity worths corresponding to these four steps will be described later along with the calculated worths.

In addition to the above mentioned standard void-worth measurements, the worth of sodium contained in the CRs and CRPs was measured relative to the 670-drawer-void configuration, which is also shown in Fig.2. These experiments were also analysed to see the applicability of our method to the prediction of the reactivity worth of sodium contained in these singularity regions.

4. Calculation Method

4.1 Preparation of Group Constants

The cross section set KFKINR³⁾ was employed. For regions other than inner and outer cores, homogeneous group constants were generated with GRUCAL code⁴⁾. For both core regions, where sodium-voiding takes place, the group constants including heterogeneity correction were prepared with the aid of KAPER code⁵⁾. This code takes into account the heterogeneity effect both on self-shielding factor and inner-cell flux which is used for cell averaging of the group constants. Details of the calculational method employed in the KAPER code are given in reference 5 and also in 6. Plate-wise heterogeneity of the control rod was not taken into account in the present study.

4.2 Cell Model

Figures 3 and 4 show the structure of as-build core cells and the calculational model used in KAPER run. In modelling for the calculation, the sodium-containing-can and the sodium-meat were treated as separate regions, though the Pu-fuel-can and the Pu-fuel were smeared into one region. Atomic number densities for each region are described in Tables 2-6. These plate-wise atomic densities were taken essentially from a data set for ZPPR-4 analysis by Pilate and de Wouters⁷⁾. Additional information from an American¹⁾ and a Japanese report⁸⁾ were consulted concerning the sodium-can and the Pu-Al plate atomic densities not available in the Belgian data. To see the consistency of the above mentioned plate-wise atomic densities, these are smeared into homogenized atomic number densities (in column "homogenized" of Table 2-6) so that one can compare them with homogeneous atomic number densities given in the original ANL-RDP report²⁾. No significant discrepancy can be found between these two sets of homogenized atomic densities.

Generally speaking, the reduction of a really three-dimensional cell into a one-dimensional calculational model is a problem of fairly delicate nature⁹⁾. Although, in the present study, no special consideration has been made on that point, the validation of that modelling procedure may deserve a detailed study especially in the light of its impact on the sodium-void reactivity effect. Specifically, the density of the steel in voided slot regions depends on the way of modelling of the cell, and it may affect the calculated void-worth.

4.3 Diffusion Coefficients

In ZPPR-3 sodium-void experiments, sodium in CRs (control rods) and in CRPs (control rod positions or sodium followers) is removed concurrently with the fuel region surrounding them. This may cause difficulties in reactor calculation when the diffusion approximation is applied. Specifically, the diffusion coefficient in CRP regions becomes unacceptably large⁸⁾ after the voiding of sodium because of the very low density of the material left after the voiding. To mitigate this difficulty, an expression for a modified diffusion coefficient by Seki and Sasaki¹⁰⁾ was used here together with the conventional $D (=1/3\Sigma_{tr})$. The former describes the neutron streaming in a channel of low material density.

The expression is relatively simple, say

$$D_z = \frac{1}{3} \{ \lambda \exp(-2a/\lambda_0) + \lambda_0 [1 - \exp(-2a/\lambda_0)] \}, \quad (1)$$

where λ and λ_0 are the neutron mean-free-paths of the surrounding material (or fuel in the present case), and of the dilute cylinder (here, normal or voided CRP), respectively, and a is the radius of the cylinder. This expression is an extension of Laletin's D ¹¹⁾. Laletin gives $D_z = \frac{1}{3}(\lambda + 2a)$ for a completely voided channel. On the other hand D_z becomes $\lambda/3$ when the channel is filled with the same material as the surrounding region. Seki et al. simply interpolated D_z between the above two extreme cases, and checked the validity of the interpolation formula by

comparisons with accurate S_N results. It has no complete firm theoretical basis, but is easy to handle because of its simplicity. As we will see later on, calculations were performed by using the conventional $D (=1/3\Sigma_{tr})$ and the modified D_z described now, and both results are compared.

Although this expression applies to neutron leakage through the Z-direction, namely, the parallel direction to the axis of the cylinder, we used the same expression for all three, say, X-, Y-, and Z-directions. This may be justified because the Z-direction leakage usually is predominant as far as the neutron streaming through the CRP region is concerned. More specifically, in Z-direction a neutron may travel for a fairly long distance through a CRP losing its importance largely. On the other hand, in X- or Y-direction, the neutron flux and importance do not differ so largely on the apposing end-sides of the CRP region. Furthermore alternative choices for X- and Y-direction diffusion coefficient*) may only slightly influence the k_{eff} 's before and after the void. Comparison of the modified D with the conventional D is given in Table 7 (1). It must be noted that the energy shapes of these two D_s are quite different. As one might see from Table 7 (2) the large increase of the conventional at the high energy region is mitigated by the contribution from the surrounding area in the case of the modified D.

When the present study was done, a direction-wise treatment of the diffusion coefficients was not possible in the Karlsruhe 3 dimensional calculation system. An average of Benoist's direction-wise coefficient, then, was used for all directions, namely,

$$D = \frac{1}{3} D_{\perp} + \frac{1}{3} D_{\parallel} .$$

Benoist's diffusion coefficient tends to overestimate the leakage component of the sodium-void reactivity worths^{12),13)}. This point will be discussed later.

*) For example, an expression for D valid for the perpendicular direction to a slab slot, which is also given in ref. 10.

4.4 Reactor Calculation

The 26 group cross sections and diffusion coefficients were collapsed into 16 groups. The first 15 of the 16 groups are of the same energy structure as the first 15 of the original 26 groups. The last 11 original groups (from 16 to 26) were collapsed into one group using spectra from a one-dimensional diffusion calculation. The calculational model is given in Fig.5. The 16-th group covers the range from the thermal energy to 0.465 KeV. Contribution from this energy range to sodium-void reactivity is, however, negligibly small because of the sharp decline of the flux-level over KeV region (for example, see Fig.1 of ref.14). Therefore, in practice, a 16-group calculation may be regarded as equivalent to an original 26-group one as far as k_{eff} and sodium-void reactivity effect is concerned.

Reactor calculations were carried out in the 16 energy groups mentioned above with D3D three-dimensional (XYZ) diffusion code¹⁵⁾.

The calculational model is shown in Fig.1. Specifically, one XY mesh is taken for one drawer (5.52x5.78 cm) with an exception of the first three mesh-intervals for X-direction (2.76 cm). The total number of three-dimensional mesh-volumes is 10350 (=23x25x18) resulting in a total of 165600 space-energy mesh-intervals^{note)}.

* * * *

Note:

A typical run-time is 40 minutes (CPU) starting from a flat source guess (~25 outer iterations), which includes about 10 minute run-time for the relaxation factor computation. Required area is 3000 K, which is enough to contain all the necessary data in core memory at a time for each energy-group. Reduction of the area down to 400 K leads to an increase in CPU time of about 50% and in the cost of more than two times as large (from 1000 to 2600 DM). This is mostly due to the tremendous increase of the access time of the peripheral working discs.

Relaxation factors calculated for the normal (or void-free) core apply well for all other voided situations of the core, reducing the cost of the computations considerably. Generally, a start from a source guess calculated for a relatively similar void-pattern fairly well reduces the computation time. A typical run time starting from a source for a similar void-pattern is less than 15 minutes without the relaxation factor computation. The machine used is IBM 370/168 at the Karlsruhe Computer Center.

5. Criticality Factors

The criticality factors calculated through the present study are summarized in Table 8. Four sets of k_{eff} 's are included here corresponding to the following four calculational methods.

- 1) For fuel region: heterogeneously corrected (cell-flux weighted) constants computed with KAPER code.
For control rod positions (CRP): conventional diffusion coefficient ($D=1/3\Sigma_{tr}$)
- 2) For fuel region: heterogeneously corrected constants.
For CRP: modified diffusion coefficient by Seki, et al.¹⁰⁾
- 3) For fuel region: homogeneous (volume-weighted) constants computed with GRUCAL code
For CRP: conventional diffusion coefficient
- 4) For fuel region: homogeneous constants after REMO-correction
For CRP: conventional diffusion coefficient

All the results are based on three-dimensional diffusion calculation by D3D code in 16 energy groups.

The upper part of the table shows the calculated k_{eff} for the reference (non-void) core configuration, some necessary corrections to it, and the comparison of the corrected k_{eff} with measured one. Consistency between measured and calculated k_{eff} 's is quite satisfactory if a rather large (0.75% Δk) heterogeneity correction is applied to the homogeneous-base calculations (cases 3). The transport correction, which is also rather large, is assumed to be the same as that for ZPPR-4, and is taken from reference 16. The atomic compositions, and configuration of ZPPR-4 core¹⁷⁾ are not far from those of ZPPR-3; hence this assumption seems to be reasonable to some extent. A check on this point, however, is still open.

The use of the different diffusion coefficients (column 1 and 2) gives rise to only 0.2% difference on k_{eff} , although it changes considerably the sodium-void reactivity worth as we will see later on.

The REMO corrected k_{eff} given in Table 8 is not suitable to be discussed here, because the correction is applied only to the central part of the core, where sodium-voiding takes place.

We will comment on this later on with respect to the sodium-void worths. However, a preliminary survey based on some one-dimensional calculations suggests that the REMO correction hardly affects k_{eff} even if it was applied to the whole core region.

The middle and the lower parts of Table 8 summarizes the set of calculated criticality factors obtained through the sodium-void calculations, which will be discussed in the next chapter.

6. Sodium Void Reactivity Worth

6.1 Analysis of the Standard Sodium-Void Experiment


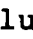


This section deals with the standard sodium-void experiment in ZPPR-3, namely, the measurement of the sodium-void reactivity worths in successively enlarged void zones. Table 9 summarizes the measured and calculated results. All are deduced from direct comparison of the calculated k_{eff} already given in Table 8. Table 9 arranges the void-worth in two ways; one in cumulative worth, and one in step-wise worth. The C/E values*) for the cumulative worths ranges from 0.69 to 1.32 when the conventional diffusion coefficient (hereafter, we denote as conventional D) being used for CRP. The use of the modified D for CRP somehow stabilizes the variation of C/E value from pattern to pattern, but increases the C/E value too much as a whole (about 35% more positive). Change in the value of D between the normal and the voided cases is larger in the conventional method as we can see in Table 7 (1), because the conventional D is an inverse of a relatively small transport cross section of the dilute CRP region. Hence, the application of the conventional D results in a less positive sodium-void worth than that obtained by using the modified D. This can be seen more clearly when one refers to the step-wise worth for the 86-drawer void pattern (⊗), which includes 6 CRPs in it. The conventional method D gives 0.15 \$ (C/E=0.35). On the other hand, the modified D method gives 0.68 \$ (C/E=1.58).


The step-wise worth for the 82-drawer pattern (⊗) is fairly well predicted by both methods. This suggests that the present method-and-data is satisfactory for the prediction of the sodium-void reactivity worth if the region considered is free of singularities. However, the 10% difference in the worths due to the different treatment of diffusion coefficient must be noted. This comes solely from the fairly large difference in the absolute value of D in both methods (see Table 7 (1)), which apply to the

*) In the case of sodium-void reactivity worth, it is generally accepted that a discussion in terms of C-E values may be more convenient. In our present case, however, the measured values do not change their signs from pattern to pattern. Hence we use C/E values conventionally.

6 CRPs just inside this annular-shaped void region. This suggests that we must be careful about the calculational method of D for the CRPs in the immediate neighbourhood even if the void region under consideration does not include any CRP.

The third method of calculating D for the CRPs was also tested, in which the D for a sodium-filled CRP was calculated in a conventional way, and a change at the removal of sodium from a CRP was calculated in the modified way; in other words D_{conv} for a sodium-filled CRP, and $D_{conv+\Delta D_{mod}}$ (voiding) for a voided CRP. The calculations were limited to the following three cases:

1) pattern  including 6 CRPs, 2) pattern , annular void just outside these 6 CRPs, which we just mentioned above, and 3) the void of sodium contained in these 6 CRPs. No essential change from the modified D case was observed. The largest change from the modified D method was seen in case 2) () , where the $D_{conv+\Delta D_{mod}}$ method yielded 0.446 $\%$ in comparison with 0.432 $\%$ by the modified D method. This suggests again a relatively high sensitivity of the void-worth for pattern  on the D applied to 6 CRPs just inside of it.

Another important fact observed from Table 9 is that the presence of CR increases C/E value by about 20% to the worse direction in comparison with the singularity-free sodium-void case as can be seen for the 60-drawer-void pattern (). We will discuss this later on. The Japanese results for the normal Phase 3 core suffer from the same kind of the discrepancy, namely, too high C/E values for some CR-including regions⁸⁾. The results by GE show about 40~50% overestimation as a whole. A separated effect from the CRs is not clear. After a correction for the group condensation effect, however, this overestimation is reported by GE to decrease down to about 35%¹⁾.

6.2 Analysis of the Reactivity Effect of Sodium Contained in Singularities (CR and CRP)

The survey in the previous section indicates that the discrepancy between the calculated void-worth and the measured one seems to be brought about essentially by the presence of singularities (CR and CRP). It is quite helpful for the further study to confirm the above statement, and to break down what is occurring. Fortunately, the measured sodium-worths in singularities are available for this purpose.

As we have already seen, the sodium-worths in CRs and CRPs were measured in the 670-drawer-void configuration, the boundary of which is shown in Fig.2. Table 10 shows the measured and calculated results in the form of sodium-void-worth (or sodium-restoring worth in opposite sign.) As one may expect from the survey on the 86-drawer void pattern (☐) in the previous section, the sodium-void worth in CRPs is too large when the modified D is used, and too small when the conventional D is used.

Here we assume that the superposition of the void worths in fuel region and in CRPs can be taken as a reasonable approximation. Exemplifying the modified D case, the void-worth of the inner 6 CRPs is overestimated by 0.204 \$ (=0.342\$-0.138\$). We subtract this 0.204\$ from the calculated void-worth (Table 9) of 86-drawer-void pattern, which includes solely these 6 CRPs as singularities. Then we get a corrected sodium-void worth of 0.476\$ or C/E value of 1.11. Through the same procedure, we get the corrected worth of 0.371\$, or C/E value of 0.86 for the conventional D case. Remarkable improvement of C/E through this simple procedure (from 1.58 to 1.11, or from 0.35 to 0.86) suggests two things: 1) Assumed superposition of sodium-void worth of the fuel region and of CRPs seems to be fairly reasonable*); 2) The large discrepancies seen in void-worth for zones which include CRPs mostly come from an inappropriate treatment of the neutron leakage through CRPs. In the same manner, we can correct the calculated worth for the maximum-void pattern (Table 9-I, last line) which includes all CRs and CRPs, because we have measured sodium-void worths for all CRs and CRPs (Table 10, second line).

*) see next page

The resulting corrected worths are 1.61% and 1.59%, for modified and conventional D cases, respectively; in terms of C/E improvement, from 1.20 to 0.94 (mod.D), or from 0.69 to 0.94 (conv. D). This notable improvement of C/E values might suggest the third fact in addition to the above two facts, say, 3) superposition of sodium-void worths of fuel and that of CRs does also work well, and the discrepancy seen in void-worths of patterns including CRs comes essentially from an inappropriate treatment of the sodium-void within the CRs. However, the following argument seems not to support the third statement.

To see the effect of the presence of CRs in a voided region, directly we examine the 60-drawer-void pattern (⊠; including solely one CR) shown in Table 9. In this case, we have no measured worth of sodium contained in the single CR considered. However, Table 10 shows the sodium-void worth in 7 CRs is over-estimated by 0.01% per one CR, namely, $(C-E)/CR=0.01\%$. We assume that this value also applies to the central single CR, and then correct the calculated sodium-void worth in the same manner as in the case of CRPs. As a result, however, the improvement of the C/E value after the correction is only minor; from 1.35 to 1.33 (mod.D), or from 1.32 to 1.30 (conv.D). This fact seems to contradict the statement 3). This argument may depend on the value of C-E for the central CR, which we inferred from the 7 CR experiment. However, even if we assume a three-times larger value of C-E for the void-worth within the central CR (i.e. 0.03% instead of 0.01%), the above argument does not change essentially. We only have a further 2% improvement of C/E value for the 60-drawer-void pattern, in which we are now interested. On the other hand, the C-E value for one CRP (not CR) only change from 0.028% to 0.034% in accordance with the position change from the outer to the inner ring. (These can be deduced from the values in Table 10). This fact may suggest that the $(C-E)/CR$ value for CRs also does not change largely from position to position, and then the factor of three adopted in the above argument may be large enough as a possible ambiguity factor. It

*) But not completely; we have concluded in the last section that we must be careful about the diffusion coefficient in CRP even when sodium-void in CRP-free zone is concerned.

may, therefore, be reasonable to say: 4) discrepancy between the measured and the calculated sodium-void worth for a zone which includes a CR region in it may come not only from an inappropriate treatment of within CR-sodium-void, but also indirectly from the surrounding fuel region through some kind of mutual influence between the fuel and the CR.

The C/E values before and after the correction described in this section are summarized in Table 11. This indicates a satisfactory prediction accuracy after the correction except the puzzling 60-drawer-void pattern with a CR in it (⊗). In the present report, the correction is carried out on the basis of the experimental information on the sodium-worths within the singularities. Even when no experimental information is available, one may probably manage to get the appropriate correction factor, especially in the case of CRPs, with the aid of a S_N or a Monte Carlo code, which allows us to estimate properly the neutron leakage effect through the CRPs.

6.3 Residual Discrepancy after Correction for Singularities

As one can see from the cumulative-worth part of Table 11, the C/E value tends to decrease with increasing of the void-volume. Specifically, we have a relatively smaller C/E value for the maximum void pattern (632-drawer-void) in comparison with the other inner-part voids. There may be two possible reasons for it at least: 1) The extension of the void-volume leads to an increase of the relative importance of the leakage component in X and Y directions, a negative contribution to the total void-worth. On the other hand, the use of Benoist's D tends to overestimate the absolute value of this component. In other words, we have a too large negative leakage component, the relative importance of which increases as the void-volume increases. Hence we have a smaller C/E value for a large void. 2) The second is phenomenological. In the previous sections, we have seen that the central 60-drawer-void worth is largely overestimated probably because of the presence of CRs in it. The influence of this unusual overestimation decreases as the void-

volume increases, because the relative contribution from this central-part void becomes smaller in the total void-worth for a larger void. This also leads to a smaller C/E value for a larger void-volume. However, we know little about the influence of the peripheral 6 CRs on the void-worth, and this is an open question. Apparently, this does not seem to cause any discrepancy, as we have rather good C/E value (0.94 after correction) for the 632-drawer-void (maximum) pattern which includes these 6 CRs in it. In the following, some additional comments are given concerning the above two points.

As is suggested in section 4.2, Benoist's D applied to the fuel cells tends to overestimate the leakage component of the sodium-void worth. Yoshida et al. concluded¹²⁾ that the overestimation is about several percent of the leakage component of sodium-void worth in the perpendicular direction to the cell platelets, and reaches about 10% in the parallel direction. Nearly the same quantitative conclusion has been reached by a different approach¹³⁾. For the case of the ZPPR-3 Phase 3 (not modified Phase 3) sodium-void, the above fact leads to several percent underestimation of void-worth for the central-part void and about 10% for the maximum-void pattern⁸⁾. Hence a part of the tendency mentioned above (especially the smaller C/E for the maximum void-pattern) may be attributed to Benoist's D applied to the fuel cells. Further, we applied the directional average of Benoist's D, say $D = \frac{1}{3}(2D_{\parallel} + D_{\perp})$, for all directions. If possible we should have applied the D_{\perp} for X and the D_{\parallel} for Y directions, respectively, or $D = \frac{1}{2}(D_{\parallel} + D_{\perp})$ for the average leakage through the X-Y plane, in which we are interested. This mismatch, stressing the D_{\parallel} component, leads to give a larger X-Y leakage component, and then decreases the C/E for the maximum void-pattern further, because the D_{\parallel} gives fairly large neutron leakage in comparison with the D_{\perp} as one can see from the nature of the neutron streaming.

The cause of the overestimation of the sodium-void worth for the 60-drawer-pattern (including one CR in center) is not clear. As an approach to this puzzle, we calculated the effect of using more realistic slowing down cross section, namely, the REMO

correction⁴⁾. No essential change, however, is seen even after the correction (Table 12). By the way, this table also suggests a merit of the use of the heterogeneously corrected group constants. The use of the homogeneous constants worsens the C/E value by 22% (from 1.19 to 1.41*) for the case of the medium-size void ($\text{U} + \text{Pu} + \text{M}$) for example.

Further, we studied the mesh-size effect for the puzzling 60-drawer-pattern. The size of the mesh was made half in the region where sodium-void takes place. As can be seen in Table 13, no essential change of the void-worth was observed by this refinement of the calculational method.

6.4 Impact of the Delayed Neutron Fraction Data

Throughout the present report up to here, we have used the value of β_{eff} taken from an original ANL-RDP report¹⁸⁾, namely 0.00301, which was adopted to convert the calculated Δk_{eff} into β unit also both in the GE¹⁾ and the Japanese⁸⁾ reports. This value is essentially based on the fast-fission data of Keepin¹⁹⁾. To get a rough idea of the impact of the recent delayed neutron data, we correct this value by simply multiplying the ratio of Tuttle's ν_d ²⁰⁾ to Keepin's ν_d to each isotope-wise contribution to β_{eff} given in ref. 18). The very small contributions from Pu 241 and Pu 242 are kept unchanged. In this way, we get a new value of 0.00323. The C/E values based on this delayed neutron fraction are also included in Tabel 11. As one can see from this table, better agreement between calculation and measurement is attained as a whole. From the view point of the delayed neutron data themselves, the new Tuttle's data seem to be more reliable²¹⁾.

*) Both after the correction for the singularities.

7. Conclusion

The general conclusions drawn from the present study are summarized in the following way.

Even in the case of a full size mockup of a prototype fast reactor, the sodium-void reactivity effect is predicted fairly well with the Karlsruhe data-and-method for singularity-free void regions. By the way, the heterogeneity correction for the core region group constants is indispensable to obtain a good accuracy.

The presence of singularities, say, control rods and control rod positions leads to some difficulties. The method adopted for the calculation of the diffusion coefficients for the control rod positions (CRPs) gives rise to a significant impact on the calculated void-worths corresponding to a pattern which contains CRPs in it. In the present study, the calculated sodium-void worths were corrected by use of the measured reactivity worths of sodium contained in CRP, and this improved the C/E values remarkably for most of the void-pattern considered. Even if no experimental data are available for CRP sodium-worth, one might be able to get some rough estimate for this correction with the aid of a S_N or a Monte Carlo code, which permits us to consider properly the neutron leakage effect through a CRP. If we want to work within the framework of the diffusion approximation, we must be careful about the diffusion coefficient for CRPs. The conventional $D(=1/3\Sigma_{tr})$ gives a too large leakage component of void-worths. The modified D by Seki et al. is better but leads to a too small leakage component. Both methods are not satisfactory, then a derivation of a more realistic D for a CRP region deserves further study. Here it should be noted that our main concern is not on the absolute value of D for a CRP but on the change of D caused by the removal of sodium, leaving only a small amount of structural material in it.

The treatment of the leakage through CRP influences, too, the accuracy of the calculated void-worths for fuel regions in the close neighbourhood of CRPs to some extent, but not so largely.

The presence of a control rod (CR) within a sodium-voided region, or most probably in the neighborhood of a fuel region undergoing sodium-void, gives rise to a severe impact on the accuracy of the calculated void-worth for the corresponding configuration. In our present case, it increases the C/E value by about 20% ($C/E = 1.35$) for a CR-containing-region void. The same procedure as the case of CRP, say, a correction based on the experimental worth of sodium contained in CRs, does not work well, indicating that the presence of CRs influences the accuracy of the calculated void-worth also for the surrounding fuel region.

The heterogeneity structure of the CR^{*)} which is not taken into account in the present analysis, might be one possible reason for this puzzling result.

Other possibilities might be among the B^{10} neutron data, or some transport effect which comes from a sharp flux change due to the presence of CR.

A use of the recent delayed neutron data instead of the old Keepin's improves the C/E values after correction for most of the void-patterns considered in this work.

Acknowledgement

The author is deeply indebted to E. Kiefhaber for continuing encouragement and fruitful discussions. The assistance offered by B. Stehle in doing D3D calculations, and by R. Kiesel and D. Woll in preparing group constants are greatly acknowledged. The author is also thankful to A. Polch, D. Thiem, G. Willerding, and N. Moritz for their help in performing calculations. Suggestions given by F. Kappler and by S. Ganesan are also appreciated.

The work was done during the author's one-year leave from Nippon Atomic Industry Group Co., Ltd., Japan.

*) The mockup CR is composed essentially of sodium- and B_4C -platelets.

Table 1: Homogeneized Atomic Number Densities for Non-fuel Regions (10^{22} atoms/cc)

	Sodium Follower (CRP)	Control Rod type A'	Control Rod type J	Radial Blanket	Axial Blanket	Reflector
composition No. (see Fig. 1)	13	14	15	16	18	17
U-235	-	-	-	0.00245	0.00156	-
U-238	-	-	-	1.108	0.7058	-
Na	1.777	1.290	0.8456	0.6377	0.8789	-
O	-	-	0.0054	2.011	1.391	-
Fe	1.002	1.125	1.183	0.8120	1.048	7.135
Cr ⁺	0.3119	0.3489	0.3648	0.2523	0.2984	0.1778
Ni	0.1323	0.1471	0.1521	0.1048	0.1237	0.05133
Si	0.01432	0.0173	0.0208	0.01177	0.01398	0.00684
Cu	0.00303	0.00300	0.00280	0.002681	0.002671	0.00126
Mo	0.00208	0.00210	0.00200	0.001928	0.001922	0.00117
C	0.00292	0.4401	0.8046	0.1015	0.003592	0.0577
Al	0.00141	0.00160	0.00290	0.001935	0.00136	0.00451
B-10	-	0.3329	0.6232	-	-	-
B-11	-	1.352	2.528	-	-	-

+) includes Mn

Table 2: Atomic Composition of Inner Core Normal Cell ($\times 10^{22}$ atoms/cc)

	Pu-U-Mo	U ₃ O ₈	Fe ₂ O ₃	Na-can	Na-meat	Matrix	homogenized	ANL-homo
Pu239	0.73418	0.0	0.0	0.0	0.0	0.0	0.08439	0.08439
Pu240	0.09772	0.0	0.0	0.0	0.0	0.0	0.01123	0.01118
Pu241	0.01129	0.0	0.0	0.0	0.0	0.0	0.00130	0.00134
Pu242	0.00158	0.0	0.0	0.0	0.0	0.0	0.00045	-
U235	0.00467	0.00301	0.0	0.0	0.0	0.0	0.00123	0.00123
U238	2.0847	1.3734	0.0	0.0	0.0	0.0	0.55534	0.55533
Mo	0.19351	0.00067	0.00067	0.005	0.00064	0.00842	0.02357	0.02357
O	0.0	3.6630	4.0972	0.0	0.0	0.0	1.31301	1.31295
Fe	1.04611	0.46946	3.1958	5.4	0.4615	3.5545	1.22991	1.22993
Na	0.0	0.0	0.0	0.0	2.0510	0.0	0.88641	0.88641
C	0.00178	0.00178	0.00178	0.015	0.0009	0.01585	0.00290	0.003
Cr	0.32321	0.14433	0.14433	1.72	0.1389	1.09900	0.25925	0.26089
Ni	0.14298	0.05885	0.05885	0.78	0.0576	0.44496	0.11894	0.11893
Si	0.01481	0.00702	0.00702	0.08	0.00650	0.04884	0.01307	0.0131
Cu	0.00281	0.00133	0.00133	0.02	0.0009	0.01414	0.00286	0.0029
Al	0.00081	0.00010	0.00010	0.003	0.00029	0.00010	0.00034	-
thick- ness (cm)	0.635	0.635	0.3175	0.0381	1.1938	0.22225		
number of plates in a unit cell		x2	x2	x4	x2	x2		

Table 3: Atomic Composition of Inner Core Spiked Cell (x10²² atoms/cc)

	Pu-U-Mo	U ₃ O ₈	Fe ₂ O ₃	Na-can	Na-meat	Matrix	Pu-Al	homogenized	ANL-homo
Pu239	0.73493	0.0	0.0	0.0	0.0	0.0	1.7496	0.18503	0.18628
Pu240	0.09787	0.0	0.0	0.0	0.0	0.0	0.08346	0.01605	0.01604
Pu241	0.01131	0.0	0.0	0.0	0.0	0.0	0.00436	0.00155	0.00160
Pu242	0.00157	0.0	0.0	0.0	0.0	0.0	0.0	0.00018	0.00018
U235	0.00467	0.00301	0.0	0.0	0.0	0.0	0.0	0.00088	0.00088
U238	2.08295	1.3722	0.0	0.0	0.0	0.0	0.0	0.39714	0.39733
Mo	0.19168	0.00066	0.00066	0.005	0.00065	0.00834	0.0047	0.02358	0.02378
O	0.0	3.6630	4.0972	0.0	0.0	0.0	0.0	1.12745	1.17168
Fe	1.0667	0.47868	3.2586	5.4	0.4773	3.6243	1.7542	1.48713	1.49258
Na	0.0	0.0	0.0	0.0	2.0509	0.0	0.0	0.88637	0.88641
C	0.00178	0.00178	0.00178	0.015	0.0010	0.01585	0.0	0.00284	0.00292
Cr	0.33178	0.14816	0.14816	1.72	0.1455	1.12813	0.4913	0.31005	0.3065
Ni	0.14710	0.06054	0.06054	0.78	0.0654	0.45777	0.2118	0.13309	0.12827
Si	0.01522	0.00721	0.00721	0.08	0.0068	0.05018	0.0	0.01300	0.01307
Cu	0.0028	0.00133	0.00133	0.02	0.0010	0.01409	0.0	0.00282	0.00287
Al	0.00087	0.00011	0.00011	0.003	0.00033	0.00011	0.18231	0.01113	0.01092
thick- ness(cm)	0.635	0.635	0.3175	0.0381	1.1938	0.22225	0.3175		
number of plates in a unit cell			x3	x4	x2	x2			

Table 4: Atomic Composition of Outer Core Type-A Cell ($\times 10^{22}$ atoms/cc)

	Pu-U-Mo	U ₃ O ₈	Fe ₂ O ₃ (inner)	Fe ₂ O ₃ (outer)	1/4 Na	1/2 Na	Na can matrix	homogenized	ANL-RDP	
Pu239	0.73484	0.0	0.0	0.0	0.0	0.0	0.0	0.0	0.16893	0.16899
Pu240	0.09788	0.0	0.0	0.0	0.0	0.0	0.0	0.0	0.02250	0.02238
Pu241	0.01131	0.0	0.0	0.0	0.0	0.0	0.0	0.0	0.00260	0.00267
Pu242	0.00161	0.0	0.0	0.0	0.0	0.0	0.0	0.0	0.00037	-
U235	0.00466	0.00301	0.0	0.0	0.0	0.0	0.0	0.0	0.00142	0.00142
U238	2.0842	1.3731	0.0	0.0	0.0	0.0	0.0	0.0	0.63695	0.63708
Mo	0.19142	0.00064	0.00062	0.00065	0.00057	0.00064	0.0005	0.00828	0.04523	0.04522
O	0.0	3.6629	4.8676	4.0970	0.0	0.0	0.0	0.0	1.45144	1.45144
Fe	1.0081	0.3756	3.8496	3.3663	0.4093	0.3915	5.4	3.7598	1.68181	1.68134
Na	0.0	0.0	0.0	0.0	1.9569	2.0446	0.0	0.0	0.63976	0.63976
C	0.00183	0.00183	0.00183	0.00183	0.0010	0.00105	0.015	0.01629	0.00310	-
Cr	0.33064	0.12287	0.12263	0.12287	0.1413	0.1315	1.72	1.2322	0.30765	0.30751
Ni	0.14752	0.04922	0.05033	0.04922	0.0609	0.0543	0.78	0.49888	0.13056	0.13050
Si	0.01527	0.00509	0.00507	0.00509	0.00645	0.0057	0.08	0.05976	0.01416	-
Cu	0.00279	0.00134	0.00134	0.00134	0.00047	0.0010	0.02	0.01384	0.00303	-
Al	0.00083	0.00011	0.00011	0.00011	0.00053	0.00031	0.003	0.00011	0.00044	-
thickness (cm)	0.635	0.635	0.3175	0.3175	0.5588	1.1938	0.0381	0.22225		
number of plates in a unit cell	x2		x2	x2			x4	x2		

1
23
1

Table 5: Atomic Composition of Outer Core Type-B Cell ($\times 10^{22}$ atoms/cc)

	Pu-U-Mo	U ₃ O ₈	Fe ₂ O ₃	Na can	1/4 Na meat	1/2 Na meat	matrix	homogenized	ANL-RDP
Pu239	0.73532	0.0	0.0	0.0	0.0	0.0	0.0	0.08452	0.08452
Pu240	0.09779	0.0	0.0	0.0	0.0	0.0	0.0	0.01124	0.01119
Pu241	0.01131	0.0	0.0	0.0	0.0	0.0	0.0	0.00130	0.00134
Pu242	0.00157	0.0	0.0	0.0	0.0	0.0	0.0	0.00018	0.00018
U235	0.00467	0.00301	0.0	0.0	0.0	0.0	0.0	0.00088	0.00088
U238	2.08539	1.3738	0.0	0.0	0.0	0.0	0.0	0.39761	0.39761
Mo	0.19369	0.00067	0.00067	0.005	0.00058	0.00066	0.00843	0.02365	0.02364
O	0.0	3.6634	4.0977	0.0	0.0	0.0	0.0	0.89208	0.89207
Fe	1.0687	0.47959	3.2648	5.4	0.3363	0.4789	3.6312	1.30983	1.30983
Na	0.0	0.0	0.0	0.0	1.9512	2.0551	0.0	1.08554	1.08557
C	0.00183	0.00183	0.00183	0.015	0.0011	0.0010	0.01629	0.00311	0.00292
Cr	0.3328	0.14861	0.14861	1.72	0.0994	0.1462	1.1316	0.28423	0.28428
Ni	0.1473	0.06061	0.06061	0.78	0.0425	0.0608	0.45825	0.13059	0.13058
Si	0.01539	0.00729	0.00729	0.08	0.0037	0.0069	0.05074	0.01419	0.01422
Cu	0.00288	0.00137	0.00137	0.02	0.0027	0.0011	0.01451	0.00339	0.00301
Al	0.00084	0.00011	0.00011	0.003	0.00042	0.00031	0.00011	0.00043	0.00043
thickness (cm)	0.635	0.635	0.3175	0.0381	0.5588	1.1938	0.22225		
number of plates in a unit cell			x2	x6		x2	x2		

Table 6: Atomic Composition of Outer Core Type-B Spiked Cell ($\times 10^{22}$ atoms/cc)

	Pu-U-Mo	Fe ₂ O ₃	Na can	1/4 Na meat	1/2 Na meat	Pu-Al	matrix	homogenized	ANL-RDP
Pu239	0.73532	0.0	0.0	0.0	0.0	1.7496	0.0	0.18507	0.18641
Pu240	0.09783	0.0	0.0	0.0	0.0	0.08346	0.0	0.01604	0.01605
Pu241	0.01122	0.0	0.0	0.0	0.0	0.00436	0.0	0.00154	0.00160
Pu242	0.00157	0.0	0.0	0.0	0.0	0.0	0.0	0.00018	-
U235	0.00465	0.0	0.0	0.0	0.0	0.0	0.0	0.00053	0.00053
U238	2.08456	0.0	0.0	0.0	0.0	0.0	0.0	0.23960	0.23961
Mo	0.19142	0.00066	0.005	0.0068	0.00032	0.0047	0.008328	0.02409	0.02384
O	0.0	4.0981	0.0	0.0	0.0	0.0	0.0	0.70656	0.75081
Fe	1.087	3.3210	5.4	0.3548	0.4930	1.7542	3.6937	1.56794	1.57248
Na	0.0	0.0	0.0	1.9512	2.0551	0.0	0.0	1.08554	1.08557
C	0.00183	0.00183	0.015	0.0011	0.0010	0.0	0.01629	0.00300	-
Cr	0.34024	0.15194	1.72	0.1068	0.1520	0.4913	1.1569	0.31020	0.30602
Ni	0.15090	0.06207	0.78	0.0461	0.0634	0.2118	0.46932	0.14232	0.13993
Si	0.01575	0.00746	0.08	0.00410	0.0072	0.0	0.05194	0.01411	-
Cu	0.00288	0.00137	0.02	0.00047	0.0011	0.0	0.01451	0.00351	-
Al	0.00086	0.00011	0.003	0.00044	0.00033	0.18231	0.00011	0.01092	-
thickness (cm)	0.635	0.3175	0.0381	0.5588	1.1938	0.3175	0.22225		
number of plates in a unit cell		x3	x6		x2		x2		

Table 7(1): Diffusion Coefficients for Control Rod Position (Na Follower) (in cm)

group no. (ABN structure)	upper group limit (eV)	modified D (by Seki et al.)			conventional D ($= 1/3 \sum_{tr}$)			$\Delta D_c - \Delta D_m$
		Sodium in	Sodium out	difference ΔD_m	Sodium in	Sodium out	difference ΔD_c	
1	10.5x10 ⁶	5.662	6.870	1.208	7.180	13.370	6.190	4.98
2	6.5 "	5.103	6.292	1.189	6.332	11.680	5.348	4.16
3	4.0 "	4.652	5.826	1.174	5.715	10.565	4.850	3.68
4	2.5 "	4.063	5.654	1.591	4.693	10.985	6.292	4.70
5	1.4 "	3.401	5.301	1.900	3.923	12.521	8.598	6.70
6	8.0x10 ⁵	3.135	5.078	1.943	3.592	12.262	8.670	6.73
7	4.0 "	2.940	4.564	1.624	3.408	9.503	6.095	4.47
8	2.0 "	2.696	4.014	1.318	3.055	6.755	3.700	2.38
9	1.0 "	2.428	3.749	1.321	2.694	6.048	3.354	2.03
10	4.65x10 ⁴	2.410	4.155	1.745	2.661	8.140	5.479	3.73
11	2.15 "	1.917	3.183	1.266	2.013	4.383	2.370	1.10
12	1.0 "	1.007	1.613	0.606	1.011	1.689	0.678	0.13
13	4.65x10 ³	0.338	2.356	2.018	0.338	2.954	2.616	0.60
14	2.15 "	1.331	2.493	1.162	1.347	2.974	1.627	0.47
15	1.0 "	1.680	2.245	0.565	1.744	2.525	0.781	0.22
16	4.65x10 ²	1.626	2.096	0.470	1.682	2.307	0.625	0.16
17	2.15 "	1.590	2.040	0.450	1.644	2.235	0.591	0.14
18	1.0 "	1.577	2.019	0.442	1.633	2.215	0.582	0.14
19	46.5	1.573	2.016	0.443	1.628	2.209	0.581	0.14
20	21.5	1.565	2.006	0.441	1.623	2.206	0.583	0.14
21	10.0	1.563	2.011	0.448	1.613	2.195	0.582	0.13
22	4.65	1.558	2.013	0.425	1.599	2.178	0.579	0.15
23	2.15	1.535	1.981	0.446	1.580	2.154	0.574	0.13
24	1.0	1.489	1.908	0.419	1.556	2.122	0.566	0.15
25	0.465	1.440	1.834	0.394	1.521	2.075	0.554	0.16
26	0.215	1.285	1.649	0.364	1.329	1.794	0.465	0.10

Table 7(2): Diffusion Coefficient of CRP (Na out) and of the Surrounding Fuel Region (in cm)

group No. (ABN structure)	upper group limit (eV)	D in voided CRP (= $\lambda_o/3$)	D in surrounding fuel region (= $\lambda /3$)	D_z^* by Seki's method
1	10.5x10 ⁶	13.370	4.435	6.870
2	6.5 "	11.680	3.925	6.292
3	4.0 "	10.565	3.477	5.826
4	2.5 "	10.985	3.134	5.654
5	1.4 "	12.521	2.380	5.301
6	8.0x10 ⁵	12.262	2.099	5.078
7	4.0 "	9.503	1.776	4.564
8	2.0 "	6.755	1.609	4.014
9	1.0 "	6.048	1.403	3.749
10	4.65x10 ⁴	8.140	1.420	4.155
11	2.15 "	4.383	1.217	3.183
12	1.0 "	1.689	0.746	1.613
13	4.65x10 ³	2.954	0.431	2.356
14	2.15 "	2.974	0.962	2.493
15	1.0 "	2.525	1.015	2.245
16	4.65x10 ²	2.307	0.976	2.096
17	2.15 "	2.235	0.928	2.040
18	1.0 "	2.215	0.877	2.019
19	46.5	2.209	0.885	2.016
20	21.5	2.206	0.829	2.006
21	10.0	2.195	0.918	2.011
22	4.65	2.178	1.018	2.013
23	2.15	2.154	0.905	1.981
24	1.0	2.122	0.535	1.908
25	0.465	2.075	0.199	1.834
26	0.215	1.858	0.240	1.649

* $D_z = \frac{1}{3} \{ \lambda \exp(-2a/\lambda_o) + \lambda_o (1 - \exp(-2a/\lambda_o)) \}$; $a = 6.38$ cm

Table 8: Summary of Criticality Factors of ZPPR-3 Modified Phase-3 Core

	heterogeneously corrected cross section (KAPER)		homogeneous cross section (GRUCAL)	
	D(CRP)=1/3 Σ_{tr}	D(CRP) by Seki	D(CRP)=1/3 Σ_{tr}	D(CRP)=1/3 Σ_{tr} Remo correction
I. normal core:				
keff: diffusion	0.99280	0.99477	0.98531	0.98556
Δk : hetero ⁺	-	-	0.00749	-
Δk : transport*	0.009	0.009	0.009	-
corrected keff	1.00180	1.00377	1.00180	-
measured keff	1.00119	1.00119	1.00119	-
C/E	1.00061	1.00258	1.00061	-

II. Voided core; keff (diffusion, without any correction): (void pattern, see Fig. 2)				
☒	0.99504	0.99706	0.99026	0.99055
+ ☐	0.99549	0.99910	-	-
+ ☑	0.99691	1.00040	-	-
+ □	0.99632	1.00090	-	-

III. measurements of sodium worth in CR's and CRP's; keff (see above)				
reference	0.99595	1.00047	-	-
Na restored in CRs and CRPs	0.99669	0.99869	-	-
Na restored in CRs		0.99958	-	-
Na restored in Inner CRP Ring		0.99944	-	-

+) difference in keff's between column 3 and 1

*) assumed to be the same as the heterogeneity correction for ZPPR-4 assembly (from Ref. 16)

**Table 9: Sodium-Void Reactivity Worths in ZPPR-3 modified Phase 3 core
Based on Three-Dimension Diffusion in 16 Energy Groups**

I. Cummulative Worths

void pattern and number of void-drawers	singularities ⁺ in voided zone	measured worths (in β unit)*	calculated void-worths in β (C/E)			
			$D(CRP)=1/3\epsilon_{tr}(CRP)$	$D(CRP)$ by Seki et al.	US results 3 dim.diff.6 gr.	
■ 42	1 CR	0.417±0.022	-	-	0.64	(1.52)
⊠ 60(42+18)	"	0.567±0.024	0.750±0.016 ⁺⁺ (1.32)	0.765±0.018(1.35)	-	-
+ ▨ 146(60+86)	1 CR + 6 CRPs	0.997±0.022	0.900±0.018 (0.90)	1.446±0.025(1.45)	-	-
+ ▩ 228(146+82)	"	1.399±0.019	1.375±0.025 (0.98)	1.880±0.025(1.34)	1.97	(1.41)
+ □ 632(228+404) (maximum)	7 CRs + 12 CRPs	1.709±0.010	1.178±0.018 (0.69)	2.048±0.022(1.20)	1.71	(1.51)

*) $\beta_{eff} = 0.00301$ (1), 18)

+) CR: control rod, CRP: sodium follower (control rod position)

++) maximum calculational error from convergence criterion; in reality the error most probably will be smaller

II. Step-wise Worth

void pattern and number of void-drawers	singularities in voided zone	measured worths (in β unit)	calculated void-worths in β (C/E)			
			$D(CRP)=1/3\epsilon_{tr}(CRP)$	$D(CRP)$ by Seki et al.		
⊠ 60	1 CR	0.567±0.024	0.750±0.016 (1.32)	0.765±0.018 (1.35)		
▨ 86	6 CRPs	0.430±0.016	0.150±0.017 (0.35)	0.680±0.026 (1.58)		
▩ 82	no	0.403±0.006	0.474±0.027 (1.18)	0.432±0.030 (1.07)		







Table 10: Sodium Void Worth in CRs and CRPs (in \$ unit)

	measured worth	calculated worth ((C-E)/voided drawer)	
		D(CRP) by Seki et al.	D(CRP)= $1/3\Sigma_{tr}$ (CRP)
Sodium in 7 CRs	+ 0.2239±0.0044	+ 0.295±0.023 ⁺ (+0.010)	+ 0.304±0.028 (+0.011)
Sodium in 7 CRs and 12 CRPs	+ 0.1507±0.0042	+ 0.588±0.015 (+0.023)	- 0.247±0.023 (-0.021)
Sodium in 12 CRPs	- 0.0732±0.0028	+ 0.296±0.018 (+0.031)	- 0.548±0.027 (-0.039)
Sodium in Inner Ring 6 CRPs	+ 0.1378±0.0082	+ 0.342±0.023 (+0.034)	- 0.083±0.023 (-0.036)

note) $\beta_{eff} = 0.00301$ 1), 18)

+) maximum possible error from convergence criterion;
in reality the error most probably will be smaller.

Table 11: Summary of C/E Values for Sodium-Void Reactivity Worths in ZPPR-3 Modified Phase 3

void pattern and number of voided drawers	measured worth (β unit)	D(CRP) = $1/3\Sigma_{tr}$ (CRP)			modified D(CRP); expression (1)			
		as calculated	corrected for CRs and CRPs		as calculated	corrected for CRs and CRPs		
I. Cumulative Worth								
 60	0.567±0.024	1.32	1.30	(1.21)*	1.35	1.33	(1.24)	
 146	0.997±0.022	0.90	1.11	(1.03)	1.45	1.23	(1.15)	
 228	1.399±0.019	0.98	1.13	(1.05)	1.34	1.19	(1.11)	
: maximum 632	1.709±0.010	0.67	0.94	(0.88)	1.20	0.94	(0.88)	
II. Step-wise Worth								
 60	0.567±0.024	1.32	1.30	(1.21)	1.35	1.33	(1.24)	
 86	0.430±0.016	0.35	0.86	(0.80)	1.58	1.11	(1.03)	
 82	0.403±0.006	1.18	1.18	(1.10)	1.07	1.07	(1.00)	

*) Values in parentheses are based on $\beta_{eff} = 0.00323$ (see section 6.4). Otherwise the value $\beta_{eff} = 0.00301$ is adopted.

When the typing of the manuscript has been finished the value of β_{eff} has been determined using the delayed neutron data usually applied at Karlsruhe and the most recent version of the corresponding evaluation routine AUDI 3. The total value is 0.00331 with the following contributions of the individual isotopes: Pu-239:Pu-240:Pu-241:Pu-242:U-235:U-238=0.00165:0.00006:0.00007:0.000003:0.00006:0.00147. The total value is only 2.5% larger than that value of 0.00323 obtained in section 6.4 of this report.

This slight difference is of no practical importance for the conclusions drawn from the present study.

Table 12: Effect of Remo Correction and of Heterogeneity
Correction on Sodium-Void Worth

calculation method	void worth ($\beta, \boxtimes + \boxplus + \boxminus$)
homogeneous constants	
before Remo correction	1.682±0.020
after Remo correction	1.669±0.027
heterogeneously corrected constants	
before Remo correction	1.375±0.025

Table 13: Effect of Mesh-size⁺⁾ on the Central Void Reactivity Worth

calculation method	void worth (β, \boxtimes)
standard mesh (~ 5.5 cm)	0.750±0.016
doubled mesh (~ 2.7 cm)	0.749±0.024

⁺⁾ Note that the mesh-size is only changed in the voided region

References

- 1) S.L. Stewart, A.K. Hartman and S.C. Crick
Evaluation and Analysis of ZPPR-3 Critical Experiments
GEAP-14001 (1974)
- 2) D.N. Olsen
Sodium-voiding Experiments in Modified Phase-3 Core
ANL-RDP-19 (1973) p.6.6
- 3) E. Kiefhaber
The KFKINR-Set of Group Constants; Nuclear Data Basis and
First Results of its Application to the Recalculation of
Fast Zero-Power Reactors
KfK 1572 (1972)
- 4) D. Woll
GRUCAL Ein Programmsystem zur Berechnung makroskopischer
Gruppenkonstanten
KfK 2108 (1975)
- 5) P.E. McGrath
KAPER - Lattice Program for Heterogeneous Critical Facilities
KfK 1893 (1973)
- 6) P.E. McGrath and E.A. Fischer
KAPER - A Computer Program for the Analysis of Experiments
Performed in Heterogeneous Critical Facilities
Paper presented at ANS Topical Meeting, 1973, Ann Arbor,
USA
- 7) S. Pilate and R. de Wouters
Data used for analysis of ZPPR-4
A letter to E. Kiefhaber (1976)
- 8) T. Kamei, T. Yoshida, K. Murakami and S. Iijima
Study on Calculational Method of Sodium Void Reactivity
Worth in Fast Breeder Reactor (II),
private communication to NEACRP meeting (June 1977)

- 9) for example, E.M. Gelbard, D.C. Wade, R.W. Schaefer and R.E. Phillips,
Nucl. Sci. Eng., 64 (1977) p.624
- 10) Y. Seki and M. Sasaki
Trans. Am. Nucl. Soc., 26 (June, 1977) p. 535
- 11) N.I. Laletin
J. Nucl. Energy, Part A, 13 (1960) p.57
- 12) T. Yoshida and S. Iijima
Journal of Nucl. Sci. and Technol., 13 (1976) p.464;
see also Appendix A to ref.⁸⁾
- 13) C.L. Beck, P.J. Collins, M.J. Lineberry and G.L. Grasseschi
On the Extrapolation of ZPR Sodium Void Measurements,
private communication to NEACRP meeting (June 1977)
- 14) E.A. Fischer
Proc. of Int. Conf. on Physics of Fast Reactors, Tokyo,
Vol.2, (1973) p. 945
- 15) B. Stehle
Ein FORTRAN-Programm zur Lösung der stationären dreidimensionalen Multigruppendiffusionsgleichungen
KfK 2118 (1975)
- 16) S. Pilate and R. de Wouters
a letter to E. Kiefhaber (1976)
- 17) J.T. Hitchcock and A.K. Hartman
Analysis of the ZPPR-4 Critical Experiments
GEAP-14077 (1976)
- 18) R.G. Palmer
P.8.14 ANL-RDP-16 (1973)

- 19) G.R. Keepin
Physics of Nuclear Kinetics, Addison-Wesley Publishing Co.,
Massachusetts (1956)
- 20) R.J. Tuttle
Nucl. Sci. Eng., 56 (1975) p.37
- 21) for example, E.A. Fischer
Nucl. Sci. Eng., 62 (1977) p.105

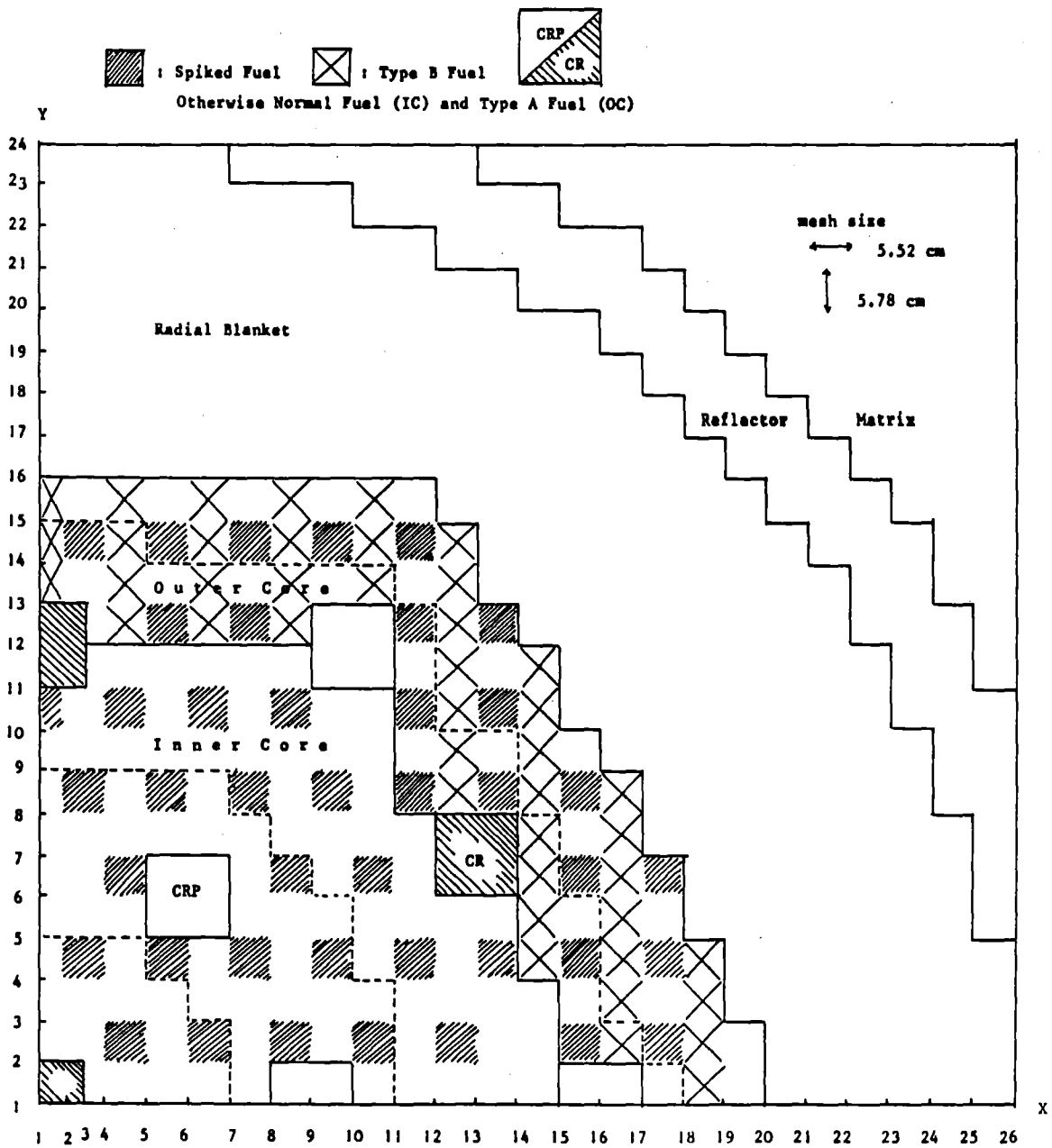
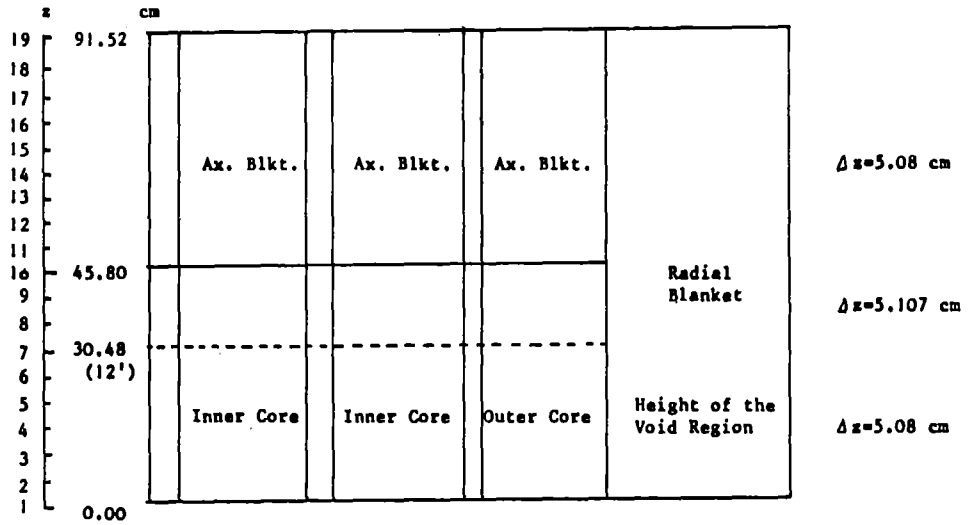


FIGURE 1 CALCULATIONAL MODEL OF Z P P R ASSEMBLY 3 MODIFIED PHASE 3 CORE

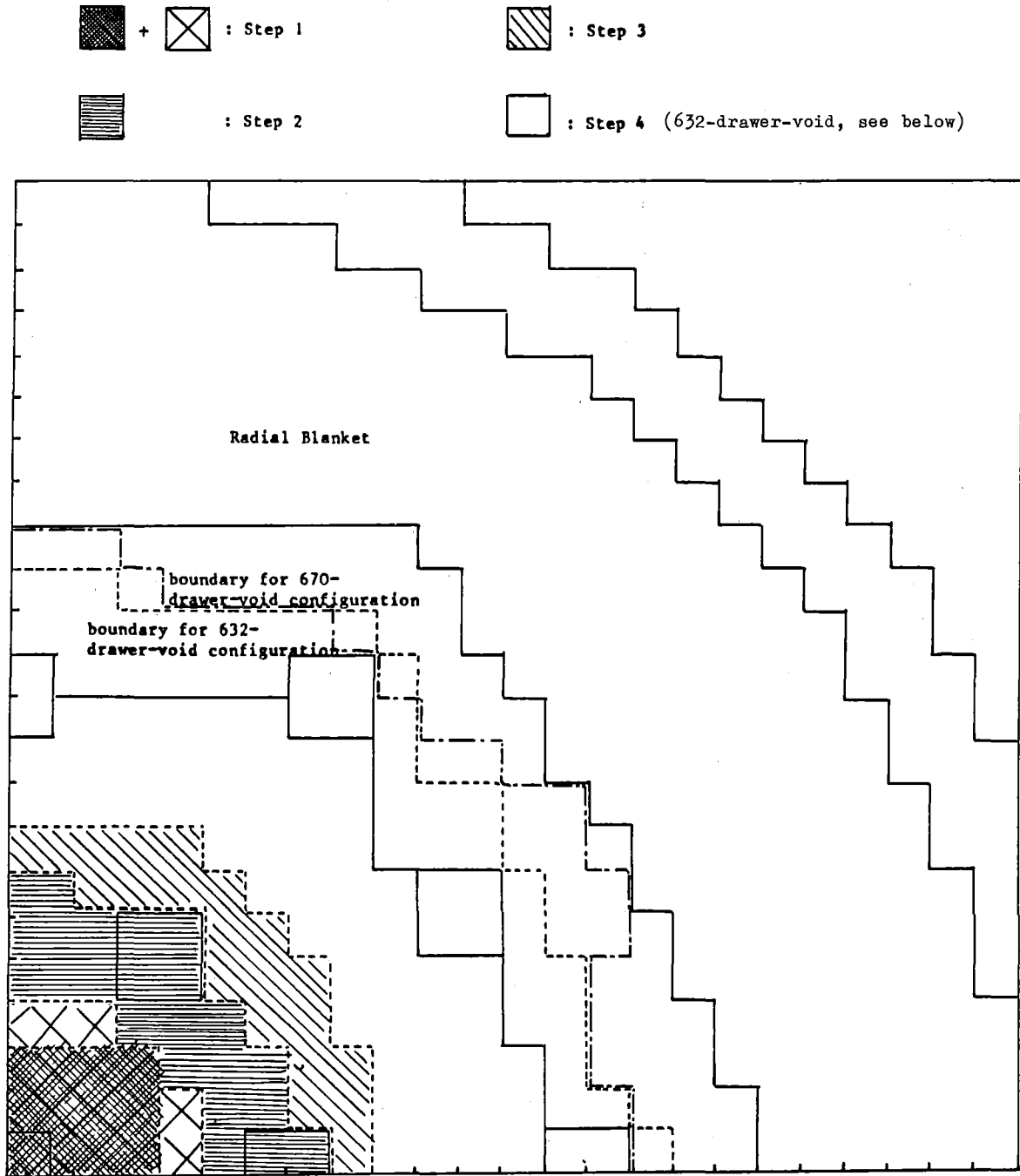


FIGURE 2 SODIUM-VOID PATTERNS SELECTED FOR THE PRESENT ANALYSIS

I. Normal I.C. Fuel, As Built

matrix
1/4 U ₃ O ₈
steel can

1/2 Na meat

steel can

1/8 Fe ₂ O ₃
steel can

1/4 Pu-U-Mo

steel can

1/8 Fe ₂ O ₃
steel can

1/2 Na meat

steel can

1/4 U ₃ O ₈

matrix

Present Calculational Model

matrix
1/4 U ₃ O ₈
steel can

1/2 Na meat

steel can

1/8 Fe ₂ O ₃

1/4 Pu-U-Mo

1/8 Fe ₂ O ₃
steel can

1/2 Na meat

steel can

1/4 U ₃ O ₈

matrix

II. Spiked Fuel, Present Calculational Model

matrix
1/4 U ₃ O ₈
steel can

1/2 Na meat

steel can

1/8 Fe ₂ O ₃

1/4 Pu-U-Mo

1/8 Fe ₂ O ₃
steel can

1/2 Na meat

steel can

1/8 Fe ₂ O ₃

1/8 Pu-Al

matrix

FIGURE 3 STRUCTURE OF THE INNER CORE FUEL CELLS

I. Type A Fuel, As Built

matrix
1/8 Fe ₂ O ₃
steel can
1/4 Pu-U-Mo meat
steel can
1/8 Fe ₂ O ₃
steel can
1/2 Na meat
steel can
1/4 U ₃ O ₈
steel can
1/4 Na meat
steel can
1/8 Fe ₂ O ₃
steel can
1/4 Pu-U-Mo meat
steel can
1/8 Fe ₂ O ₃
matrix

Present Calculational Model

matrix
1/8 Fe ₂ O ₃
1/4 Pu-U-Mo
1/8 Fe ₂ O ₃
steel can
1/2 Na meat
steel can
1/4 U ₃ O ₈
steel can
1/4 Na meat
steel can
1/8 Fe ₂ O ₃
1/4 Pu-U-Mo
1/8 Fe ₂ O ₃
matrix

II. Type B Fuel, As Built

matrix
steel can
1/2 Na meat
steel can
1/8 Fe ₂ O ₃
steel can
1/4 Pu-U-Mo meat
steel can
1/8 Fe ₂ O ₃
steel can
1/2 Na meat
steel can
1/4 U ₃ O ₈
steel can
1/4 Na meat
steel can
1/4 Na meat
steel can
1/4 Na meat
steel can
1/4 Na meat
steel can
matrix

Present Calculational Model

matrix
steel can
1/2 Na meat
steel can
1/8 Fe ₂ O ₃
1/4 Pu-U-Mo
1/8 Fe ₂ O ₃
steel can
1/2 Na meat
steel can
1/4 U ₃ O ₈
steel can
1/4 Na meat
steel can
1/4 Na meat
steel can
matrix

III. Type B Spiked Fuel, Present Calculational Model

matrix
steel can
1/2 Na meat
steel can
1/8 Fe ₂ O ₃
1/4 Pu-U-Mo
1/8 Fe ₂ O ₃
steel can
1/2 Na meat
steel can
1/8 Fe ₂ O ₃
Pu-Al
steel can
1/4 Na meat
steel can
matrix

FIGURE 4 STRUCTURE OF THE OUTER CORE FUEL CELLS

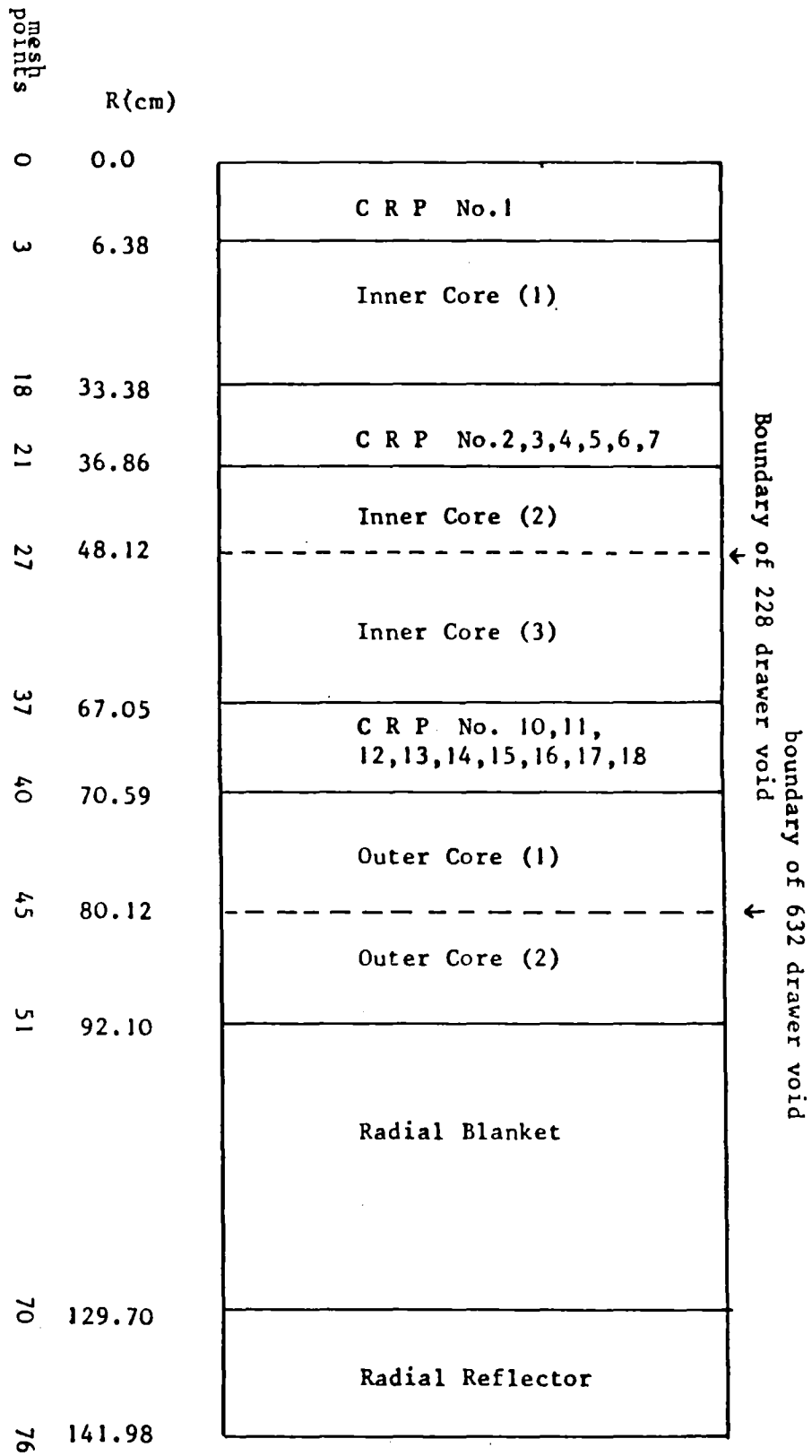


FIGURE 5 ONE-DIMENSIONAL REACTOR MODEL OF ZPPR3 PHASE3 (MODIFIED)